EVALUATING THE MECHANICAL PROPERTIES OF FIBERGLASS-REINFORCED POLYMER BAR

ABSTRACT

This study examined the mechanical characteristics of glass fiber-reinforced polymer (GFRP) bars following its introduction in the Ghanaian construction industry. Tensile strength, tensile failure strain, and modulus of elasticity for different GFRP bar diameters were examined. The specimens were investigated according to the provisions in the British Standards. To conduct the tensile strength test on the GFRP, a gripping technique was required to prevent slippage or premature failure. The gripping mechanism comprised a circular steel pipe with an inner diameter of 22mm and 150mm long for gripping on both ends of the specimen where 150mm long of the GFRP bar was implanted into the steel pipe, leaving 300mm of free length. Thus, an appropriate embedment length and adequate pipe size were crucial components in this kind of gripping device. An epoxy mixture with expanding additives and high-strength non-shrink was used to fill the area between the steel pipe and the bar. The GFRP bar sizes used in this test were 10mm, 12mm, and 16mm and their tensile strength from the test results were 1193 N/mm², 1030 N/mm², and 866N/mm² respectively. The modulus of elasticity of the fiberglass also varied for the10mm, 12mm, and 16mm as 54434 MPa (N/mm²), 41711 MPa (N/mm²), and 30516 MPa (N/mm²) respectively. The ultimate strain for 10mm, 12mm, and 16mm was 2.20%, 2.48%, and 2.8% respectively. The measured values of ultimate strength, failure stresses, and axial tensile modulus correspond well with the values published in the relatively limited available literature. From the experimental data, the stress-strain relationship for all bar sizes was a single monotonic straight line. Thus, failure of the bars occurred suddenly without the warning that is usually associated with ductility beyond ultimate/maximum stress. Compared to conventional steel, fiber-reinforced polymers are highly robust and lightweight. Its

mechanical properties, however, are linear elastic and lack a prominent yielding stage, which lowers the rates of elongation and failure strain. Furthermore, GFRP usually has a lower elastic modulus than steel, and unlike steel is non-homogeneous and an-isotropic.

KEYWORDS: Glass fiber; tensile strength; modulus of elasticity; stress and strain; factor of safety

INTRODUCTION

Fiber Reinforced Polymer (FRP) bars have become increasingly popular in concrete structures due to their advantages over conventional steel reinforcement. These days, with development happening so quickly, it can be difficult to obtain structural materials like steel and wood. Societies generally encourage the use of recyclable materials, and numerous researches have been carried out to solve the scarcity of material supply. Materials have been combined in different ways to increase the reinforcement's contribution to construction (Arya et al. 2005). Reinforced with Fiber in civil engineering and other fields, the polymer is a composite material made of cement mix, fine and coarse aggregates, and discrete, discontinuous, uniformly dispersed appropriate fibers like steel, glass, and natural fibers, among others. Because conventional concrete has a low tensile strength, it can only absorb limited energy if it is used alone without reinforcement. The weakness in the tension zone can be remedied by adding fiber elements that reinforce the cement concrete matrix. Using fibers in concrete can increase the material's compressive strength, tensile strength, and Young's modulus of elasticity. For efficient stress transfer, the FRP-to-concrete interface's performance is essential (Teng et al., 2006). The demand for strong, resilient, and stiff materials that might take the place of traditional civil engineering materials in harsh conditions led to the development of FRP composites as a structural material in the middle of the 1980s (Zaman et al., 2013). In addition to its presence in reinforced concrete (RC) structures, FRP reinforcement has been used in timber structures for purposes of reinforcement and repair. The bonding of FRP attached to wood constructions using adhesives offers advantages, but the absence of formalized design guidelines has limited its use (Schober et al., 2015). The mechanical properties of FRP bars play a crucial role in their application as reinforcement in concrete structures. FRP bars offer several

advantages over steel reinforcement, including high tensile strength, low modulus of elasticity that leads to large strains within the linear stress-strain response, corrosion resistance, and fatigue endurance (Li et al., 2017). Tensile strength is an important mechanical property of FRP bars with high tensile strength, which allows them to effectively resist tensile forces in concrete structures. The tensile strength of FRP bars can be as high as, or even higher than that of steel reinforcement (Li et al., 2017). This high tensile strength makes FRP bars suitable for applications where superior corrosion resistance and strength are required, such as in seawalls, bridge decks, pavements exposed to deicing salts, and deep beams (Li et al., 2017). The modulus of elasticity is another key mechanical characteristic of FRP bars. The modulus of elasticity of FRP bars is smaller than that of steel bars, which means that FRP bars are more flexible and have a lower stiffness compared to steel reinforcement (Karim et al., 2016). However, whereas GFRP usually has a lower modulus of elasticity than steel, it has been found that CFRP has a high Young's modulus of elasticity (Mansoori, 2017). This lower modulus of elasticity of reinforcing GFRP bars can affect the behavior of concrete structures particularly in terms of serviceability performance. Compared to reinforcing steel bars, GFRP bars can result in increased deflections and decreased stiffness in concrete elements, such as beams and slabs (Maranan et al., 2015).

2. MATERIALS AND METHODS

2.1 Experimental Work

The experimental work was designed to evaluate the mechanical properties of the GFRP bar. This involved sampling of different sizes of GFRP bars as 10mm, 12mm, and 16mm to study the various properties of the bar.

2.2 Specimen Preparation

The GFRP bars used in this investigation are potential substitutes for reinforcing steel bars which are made by pultruding impregnated thermoset resin fibers (Ogaili et al., 2020).

Eighteen (18) GFRP specimens in three different sizes (10, 12 and 16 mm) were prepared. The designation TCBx-a was assigned to each specimen, where "x" stands for the diameter of the bar in millimeters and "a" for the number of tests. The details of test specimens are shown in Table 1.

Table 1: Samples of GFRP bar for Testing

Nominal Diameter (x)	10	12	16
Number of Samples (a)	3	3	3
Cross-Sectional Area (mm^2)	78.54	113.10	201.06

A test-bar gripping mechanism used in this work employed a 25mm circular steel pipe for 16mm,12mm, and 10mm fiberglass with an inner diameter of 22mm. At both ends, the GFRP bar was implanted 150mm into the steel pipe, leaving 300mm of free length as indicated in Figure 1. Providing an appropriate embedment length and an adequate pipe size were crucial components in this kind of gripping device. According to Castro and Carino (1998), in order to keep the bar from slipping out of the steel pipe, the embedment length should be at least 15 times the bar diameter (d). Using the grips at the bar ends was essential to tackling the issue of the GRP bars' weakness in shear resistance and helping to reduce and redistribute the high stress in the anchorage area, which would have otherwise resulted in the crushing of the bars' anchorage area.

Figure 1: Sample of the specimen with gripping.

An epoxy mixture with expanding additives and high-strength non-shrink was used to fill the area between the steel pipe and the bar. The epoxy transferred the pressure that the machine applied to the steel pipes to the surface of the GFRP bar. The epoxy chemical used was Bisphenol A. It was used due to its availability and also its variety of molecular weights.

The specimens were held vertically in place for the pouring of the epoxy into the pipes. A sealant was applied to the edges to close any excess holes. After that, a mixture of epoxy chemicals with a ratio of 2:1 (i.e. 2 parts of the resin to 1 part of the harder) was poured into the open part of the coupler. The same procedure was used to prepare the opposite end of the bar.

The epoxy took 24 hours to be fully dried. The specimens were left for a minimum of three days following the pouring process for the epoxy to harden adequately before the tensile test was conducted.

2.3 Tensile Test

The purpose of the tensile test was to ascertain the GFRP bars' elastic modulus and tensile strength., failure strain, stress, and strain curve, and also the partial factor of safety. The test was done according to BS EN 1002. A 50mm gage length extensometer was used to quantify elongation during the tension tests, which were

conducted using an ELE universal testing machine with a 1000 kN capacity. Using the Vernier calipers to the nearest 0.1 mm to measure the diameter of the bar, the cross-sectional area of a single fiber was computed.

2.3.1 Testing Procedure

The samples were subjected to a monotonically applied tension at a displacement rate of 3 mm per minute until failure was reached. The failure of the specimens was caused by either the fiberglass completely detaching from one side of the specimens or the epoxy situated between the bar and the coupler failing. The universal testing machine used in this investigation is depicted in Figure 2.

Figure 2: Tensile test setup.

3. Results and Discussions

3.1 Strength Properties and Effect of Bar Size

The average values of ultimate strength, ultimate elongation, Young's modulus of elasticity, and failure modes of the GFRP bars of size 10mm, 12mm, and 16mm are shown in Table 2. The failure mode is either GFRP ruptures, slips, or exhibits a failure of the coupler and bar to de-bond. All the test was done with attached strain gauge measurements to directly compute Young's modulus of elasticity.

Table 2: Summary of test results for 10, 12 and 16mm bars

Size	*Failure mode*	*Average Ultimate Tensile Strength (N/mm²)*	*Average Young's Modulus of Elasticity* (kN/mm^2)	*Average Ultimate Elongation (%)*
10mm	Rupture	1193	54.434	2.20
10mm	Slippage	920	53.515	1.7
12mm	Rupture	1030	41.711	2.48
12mm	Slippage	829	47.571	1.7
16mm	Rupture	866	30.516	2.8
16mm	Slippage	573	33.099	1.7

The mean and standard deviation for Young's modulus of elasticity and ultimate tensile strength for GFRP of different diameters are presented in Table 3.

Table 3: Mean and standard deviation in Young's modulus of elasticity and tensile strength for Rupture.

Diameter	10mm		12mm		16mm	
Property	Young's Modulus of elasticity (kN/mm^2)	Tensile Strength (N/mm²)	Young's Modulus of elasticity (kN/mm^2)	Tensile Strength (N/mm²)	Young's Modulus of elasticity (kN/mm^2)	Tensile Strength (N/mm²)

Mean	54.434	1193	41.711	1030	30.516	866
Standard deviation	9.467	136	4.882	57	3.170	114

Table 4: Mean and standard deviation in Young's modulus of elasticity and tensile strength for slip.

Diameter	10mm		12mm		16mm	
Property	Young's Modulus of elasticity (kN/mm^2)	Tensile Strength (N/mm^2)	Young's Modulus of elasticity (kN/mm^2)	Tensile Strength (N/mm^2)	Young's Modulus of elasticity (kN/mm^2)	Tensile Strength (N/mm^2)
Mean	53.513	920	47.571	829	33.099	573
Standard deviation	4.713	64	4.466	50	6.151	95

From the recorded results in Table 1, it is observed that when the GFRP bar size increases, its strength decreases, and for larger bars, the ultimate strength is typically lower. It can be deduced based on the test results that one main reason for the inverse relationship between strength and bar sizes is that the fiberglass is heavily sensitive to small defects and smaller diameters have a smaller chance of containing or precipitating these defects (Nawy et al., 1971). The tensile strength of different specimens of the same size differs from different bar sizes, meaning that the material is non-homogeneous and isotropic.

The relationships between the diameter and average modulus, strength, and elongation of bars for rupture and slip failure are shown graphically in Figures 3a and 3b, 4a and 4b, and 5a and 5b, respectively. The results

show a good correlation between the bar size and the tensile strength and modulus of elasticity of the GFRP bars in this study. Relationships can be drawn to predict tensile strength, modulus of elasticity, and strain from the bar diameter, and they are dependent on the type of failure mode, whether the failure mode is by rupture of the bar fibers or slippage between them. The relationships are described in Equations 1 to 3. Figures 3a, b, and 4a,b all show negative slopes while Figure 5a illustrates a relationship based on rupture failure mode on the other hand shows a positive slope between average bar strain and bar size. However, based on slippage failure mode, Fig 5b shows that the average bar strain is independent of bar size. These graphs demonstrate that the GFRP bars do not possess homogeneous properties but as the diameter increases there is a decrease in both tensile strength and modulus of elasticity. The relationships are as follows:

A. Tensile Strength (Y in N/mm^2) versus Bar diameter (X in mm)

For Rupture failure mode:

$$Y = 1695.6 – 52.57X \quad \text{Eq.1a}$$

For Slippage failure mode:

$$Y = 1517.7 – 58.714X \quad \text{Eq.1b}$$

B. Modulus of elasticity (Y in N/mm^2) versus Bar diameter (X in mm)

For Rupture failure mode:

$$Y = 90565 – 3816X \quad \text{Eq. 2a}$$

For Slippage failure mode:

$$Y = 88218 – 3433X \quad \text{Eq. 2b}$$

C. Strain (Y) versus Bar diameter (X in mm)

For Rupture failure mode:

$$Y = 0.001X + 0.0128 \quad \text{Eq.3a}$$

For Slippage failure mode:

Y = 0.00017 Eq.3b

The tensile strength and modulus of elasticity decrease with bar size. Therefore, the least bar size of 10mm produced the highest strength and modulus of elasticity among the three bar sizes. This can be explained that the smallest bar has the most robust molecular or atomic structure. Its ability to resist deformation or failure under load is most largely influenced by its internal structure and the internal forces between its constituent particles. It possesses stronger inter-molecular or inter-atomic bonds that tend to have higher strength and stiffness than the larger bars.

The tendency for the GFRP bar to crush in the machine jaws or wedges can be attributed to its relatively low strength in compression as compared to tension. Its low compressive strength makes it unsuitable for reinforcement in major structural compressive members such as columns and walls. Furthermore, its application as reinforcement will be challenged in structural concrete members that will be subjected to cyclic or reversible loads as in seismic. However, its high tensile strength should make it a favorable reinforcing material in concrete members that sustain high-impact tensile loads.

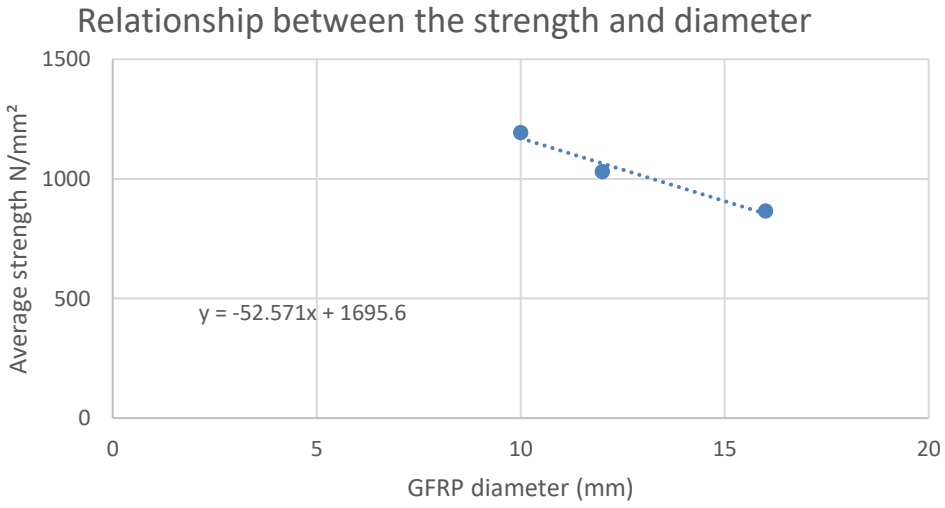

Figure 3a: Relationship between tensile strength and diameter of GFRP bar (Rupture failure)

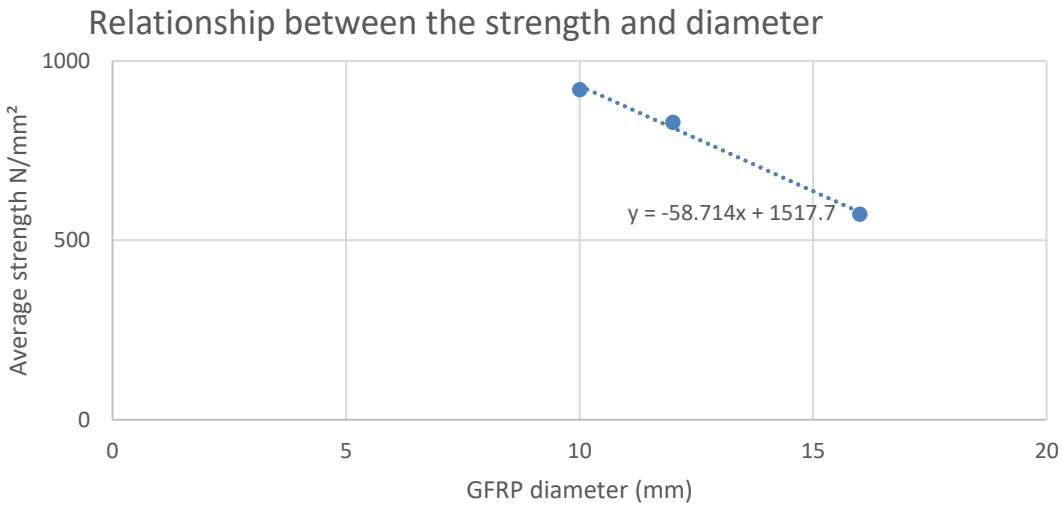

Figure 3b: Relationship between tensile strength and diameter of GFRP bar (Slippage failure)

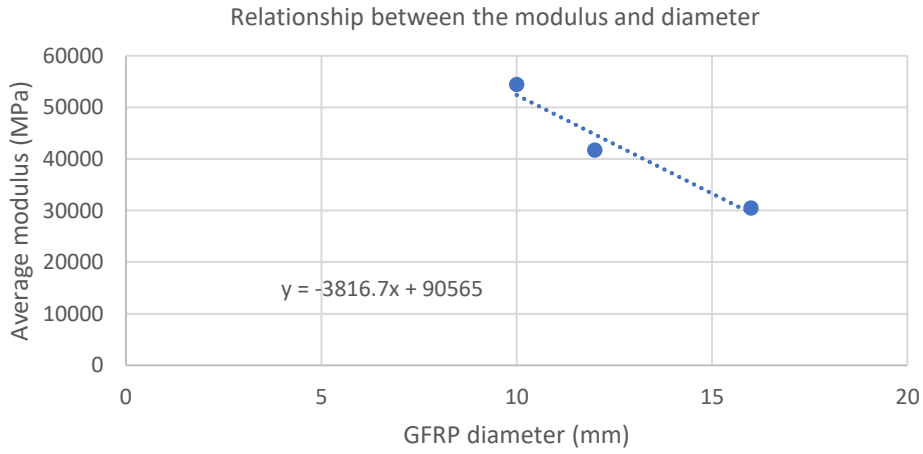

Figure 4a: Relationship between modulus of elasticity diameter of GFRP bar (Rupture failure)

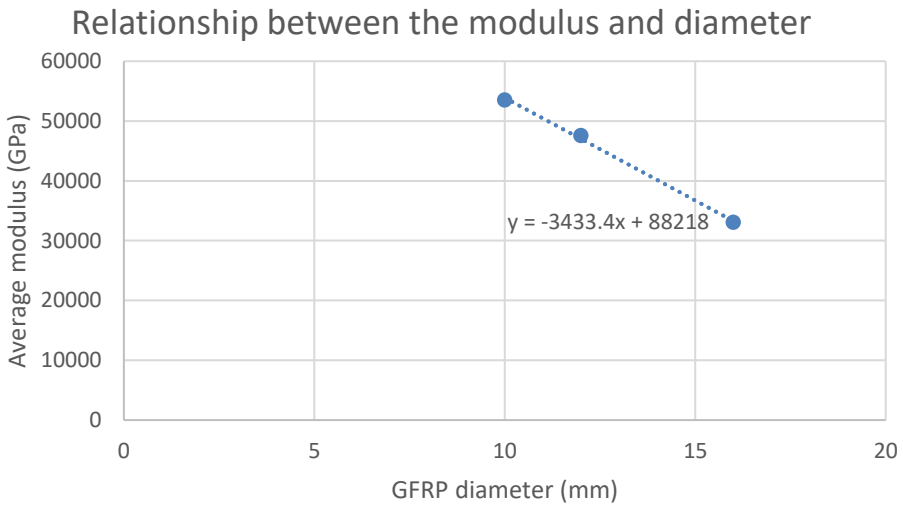

Figure 4b: Relationship between modulus of elasticity diameter of GFRP bar (Slippage failure)

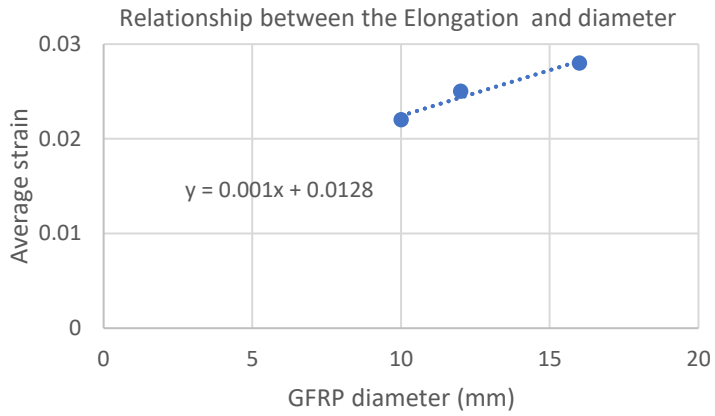

Figure 5a: Relationship between strain and diameter of GFRP bar (Rupture failure)

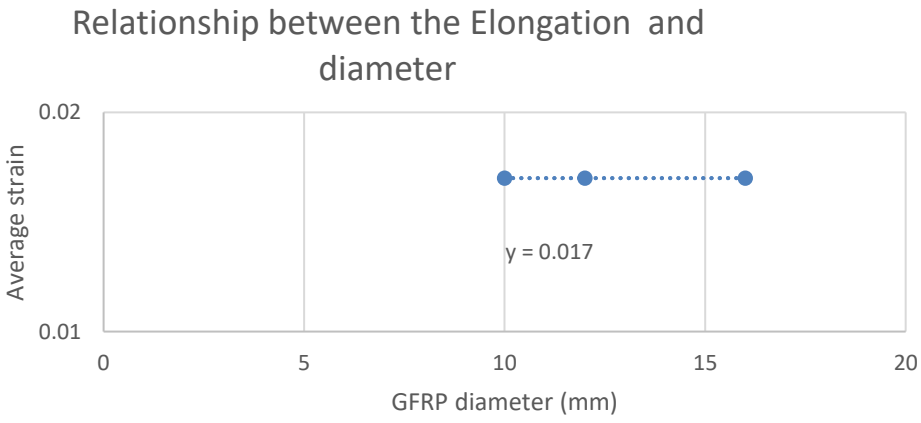

Figure 5b: Relationship between strain and diameter of GFRP bar (Slippage failure)

3.2 Stress-Strain curve

The stress-strain curves for GFRP bars of diameters 10, 12, and 16mm for both slip and rupture are shown in Figures 6, 7, and 8 respectively demonstrate that the samples exhibited a linear elastic behavior up to failure, at which point they failed suddenly without prior warning. Throughout the test, the GFRP specimens exhibited this constant behavior. The graphs show that the stress-strain relationship followed a comparatively similar trend of single and continuing linear response but of varied gradients until failure for the different GFRP bar sizes. This suggests that the glass fibers are naturally fragile. It can also be observed from the figures that the stress–strain curves overlap each other in the initial part of glass fibers, which leads to a deduction that the modulus of elasticity tends to be similar at low applied tension for all bar sizes.

There is no apparent yield point in the stress–strain curves of GFRP bars that are normally associated with steel bars that undergo combined linear and non-linear paths of their stress–strain response and are usually synonymous with ductile failure modes of structural members during which ample warning is exhibited of impending failure. Despite its lack of prominent yielding stage characteristic, the large strain capacity that is associated with a low modulus of elasticity in the entire elastic range would likely make GFRP a suitable reinforcing bar to resist high stresses such as in members subjected to explosive loads, in bridges that carry extremely heavy traffic loads and other heavy dynamic loads.

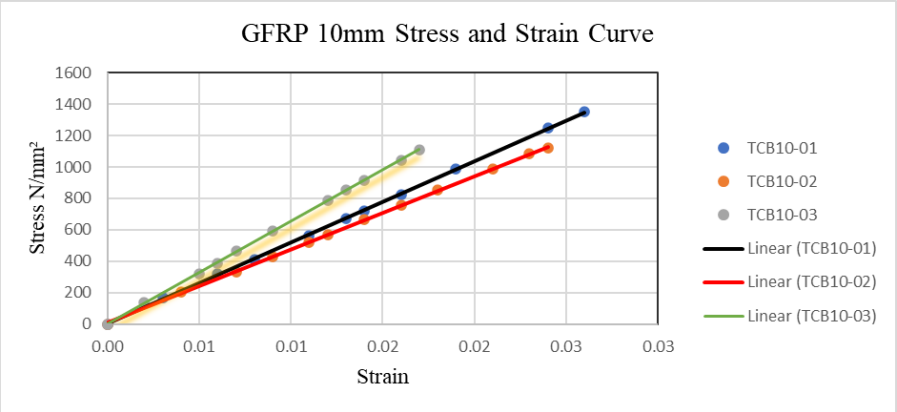

Figure 6a: Stress and strain curve for 10mm GFRP bar (Rupture failure)

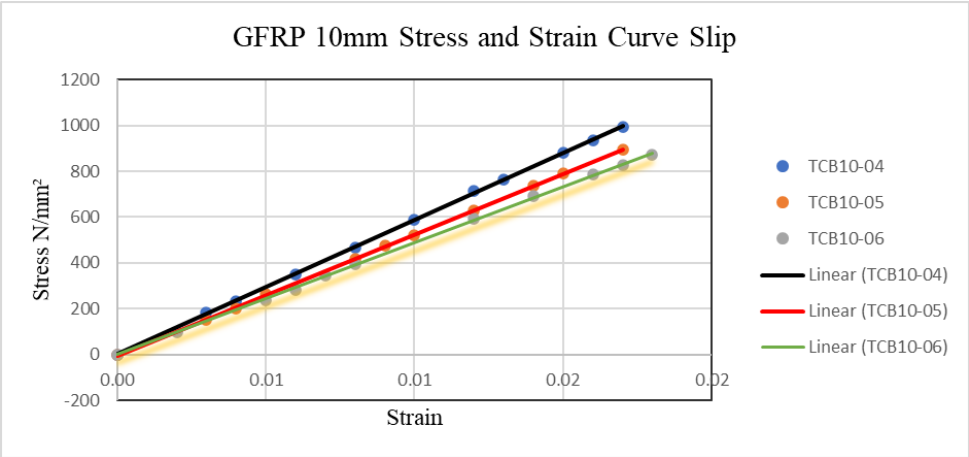

Figure 6b: Stress and strain curve for 10mm GFRP bar (slippage failure)

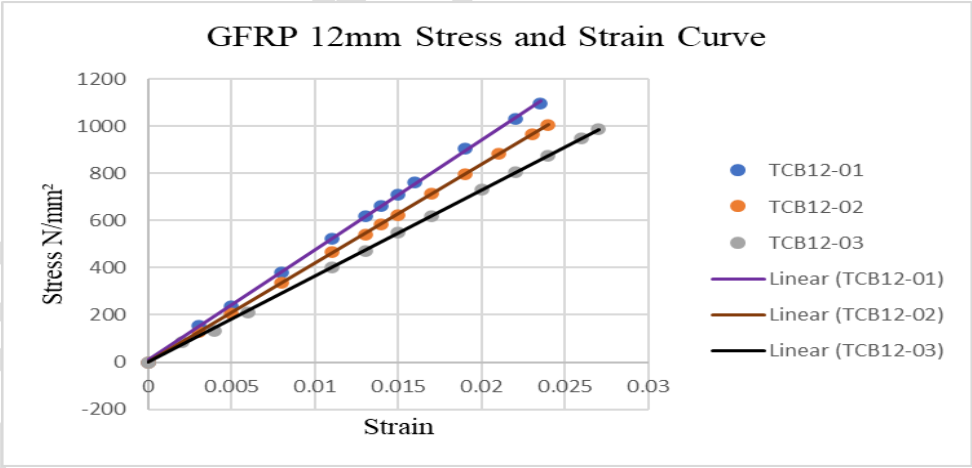

Figure 7a: Stress and strain curve for 12m GFRP bar (rupture failure)

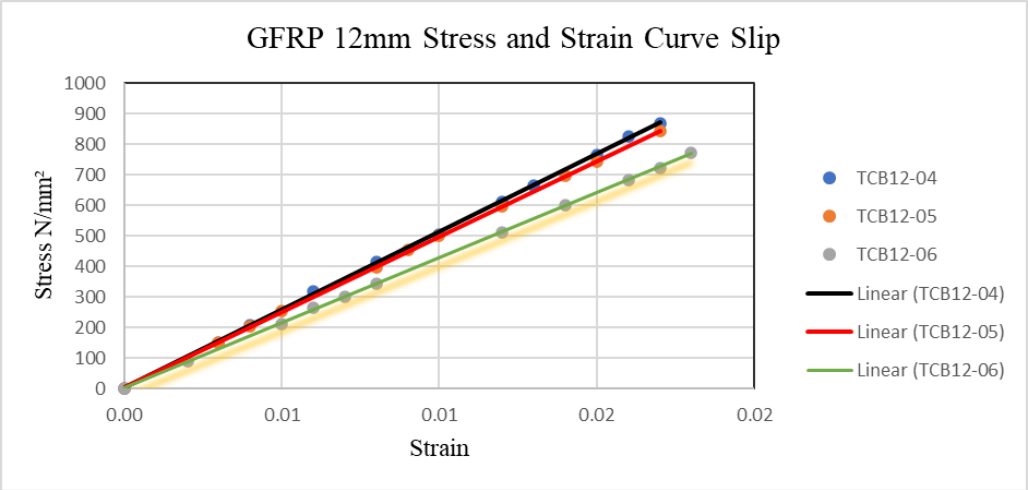

Figure 7b: Stress and strain curve for 12mm GFRP bar (slippage failure)

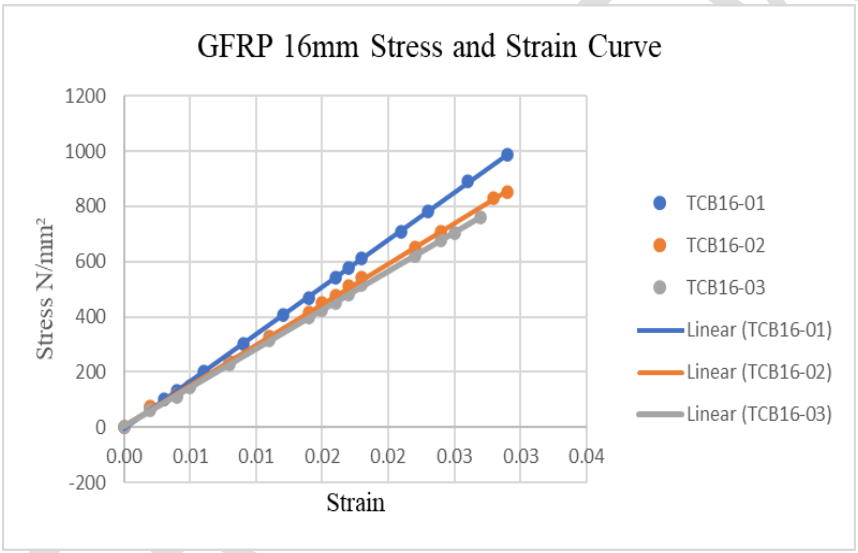

Figure 8a: Stress and strain curve for 16mm GFRP bar (rupture failure)

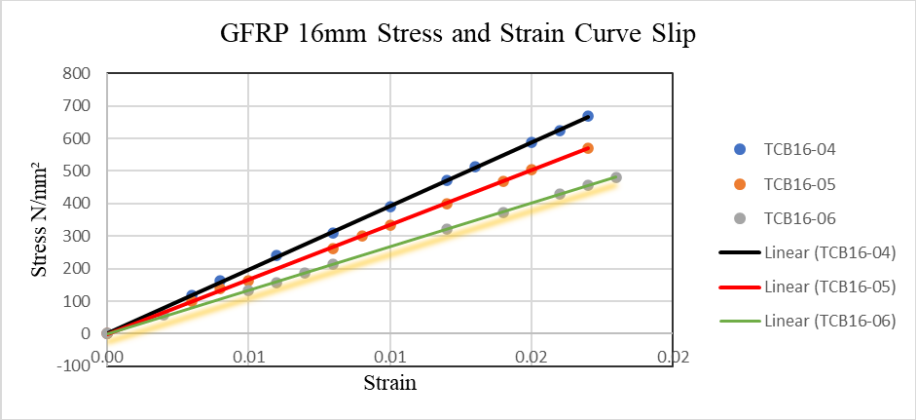

Figure 8b: Stress and strain curve for 16mm GFRP bar (slippage failure)

3.3 Partial Factor of Safety

The factor of safety for GFRP bars is not a fixed value but rather depends on several factors including the application type, loading conditions, material properties, and building codes and standards (Alsayed et al., 2000). For instance, the authors examined the effectiveness of GFRP as reinforcing bars in concrete buildings and assumed the partial factor of safety to be 1.5 for computing the design tensile strength of GFRP reinforcing bar. Another researcher, Worner (2015) investigated the use of GFRP reinforcing bars for concrete bridge decks where a partial factor of safety of 1.8 was used for GFRP reinforcing bars in the design of various experimental concrete sections. Despite the varying factors of safety values of GFRP bars, Pilakoutas et al. (2011) concluded that high factors of safety would eventually lead to concrete crushing and will not necessarily improve the safety of elements. In the midst of some differing opinions on the use of appropriate values for the factor of safety for GFRP reinforcing bars, several codes of practice recommend the material factor of safety for concrete, steel, and fiberglass as shown in Table 5 (BS EN 1990:2002 + A1, 2005; BS EN 1992-1-1,2004; FIB,2007).

Table 5: Material factor of safety (BSI, 2002; 2004 and FIB, 2007)

Material factor of safety		
γ_c	γ_s	γ_f
1.5	1.15	1.25

where:

γ_c = partial factor safety for concrete

γ_s = partial factor safety for steel

γ_f = partial factor safety for fiberglass

In summary, the commonly published values of the factor of safety for GFRP from existing literature are; found to be 1.5, 1.8, and 1.25 (Alsayed et al.,2000; Worner, 2015, BS EN 1990:2002 + A1, 2005; BS EN 1992-1-1, 2004; FIB, 2007). Based on these published values, an average value of 1.52 is recommended for use as the partial factor of safety for GFRP reinforcing bar in concrete.

4.0 Conclusions

Using the procedures stipulated in the BS EN 10002 standard, the modulus of elasticity, ultimate strength, and failure of glass fiber-reinforced polymer bars have been investigated. The GFRP bars used in this test comprising 10mm, 12mm, and 16mm have an ultimate tensile strength of 1193 N/mm², 1030 N/mm², and 866N/mm² respectively. The Young's modulus of elasticity of the GFRP is 54434 N/mm², 41711 N/mm², and 30516 N/mm² for 10mm, 12mm, and 16mm bar sizes, respectively. The ultimate strain is 2.20%, 2.48%, and

2.8% for 10mm, 12mm, and 16mm respectively. The measured values of ultimate strength, ultimate strain, and modulus of elasticity in tension correspond well with the values published in existing literature.

From the test results, it is found that the smallest bar size 10mm exhibits the highest tensile strength and highest Young's modulus of elasticity among the bar sizes. This could be because the 10mm bar has the most robust molecular or atomic structures and its ability to resist deformation or failure under load is most largely influenced by strong internal structure and forces between its constituent particles. The strength of intermolecular or interatomic bonds that tend to control both strength and stiffness increases with decreasing GFRP bar size. It is found that the stress-strain curve for all the GFRP bars has a straight line and therefore as the stress increases, the strain expectedly increases proportionally until it reaches the ultimate strength stage where failure occurs. Compared to conventional steel, fiber-reinforced polymers are highly robust and lightweight. Its mechanical properties, however, are linear elastic and lack a prominent yielding stage, which lowers the rates of elongation and failure strain. Furthermore, GFRP usually has a lower elastic modulus than steel as confirmed in existing literature. GFRP composites come in a variety of shapes, such as roving, rebar, rod, tube, sheet, beam stirrup, plate, and textile and mesh fabric, and can be used as reinforcement with concrete. The test results of this study have shown that the mechanical properties of GFRP bars are different for different specimens of the same size and also different for different bar sizes, meaning that GFRP is not homogeneous.

REFERENCES

1. Alsayed, S. H., Al-Salloum, Y. A., & Almusallam, T. H. (2000). Performance of glass fiber reinforced plastic bars as a reinforcing material for concrete structures. Composites Part B: Engineering, 31(6-7), 555-567.
2. Arya, M. H., Reis, R. L., & and L BOESEL, V. C. (2005). Material properties of biodegradable polymers. Biodegradable polymers for industrial applications, 336.
3. BSI (2002) BS EN 1990:2002+A1:2005: Eurocode: Basis of structural design. BSI, London, UK.
4. BSI (2004) BS EN 1992-1-1:2004: Eurocode 2: Design of concrete structures: part 1-1: general rules and rules for buildings. BSI, London, UK
5. Castro, P. F., & Carino, N. J. (1998). Tensile and nondestructive testing of FRP bars. Journal of composites for construction, 2(1), 17-27.
6. FIB (Fédération Internationale du Béton) (2007) FIB – TG 9.3: Technical Report: FRP

7. Karim, H., Sheikh, M., Hadi, M. (2016). Axial Load-axial Deformation Behaviour of Circular Concrete Columns Reinforced with GFRP Bars and Helices. Construction and Building Materials, (112), 1147-1157. https://doi.org/10.1016/j.conbuildmat.2016.02.219

8. Li, W., Fan, S., Ho, S., Wu, J., Song, G. (2017). Interfacial Debonding Detection In Fiber-reinforced Polymer Rebar–reinforced Concrete Using Electro-mechanical Impedance Technique. Structural Health Monitoring, 3(17), 461-471. https://doi.org/10.1177/1475921717703053

9. Mansoori, I. A. (2017). Rehabilitation of reinforced concrete haunched beam with carbon fiber reinforced polymer (CFRP) strips. *Gaziantep University*.

10. Maranan, G., Manalo, A., Benmokrane, B., Karunasena, W., Mendis, P. (2015). Evaluation Of the Flexural Strength and Serviceability Of Geopolymer Concrete Beams Reinforced With Glass-fibre-reinforced Polymer (GFRP) Bars. Engineering Structures, (101), 529-541. https://doi.org/10.1016/j.engstruct.2015.08.003

11. Nawy, E., Neuwerth, G., Phillips, C. (1971), "Behavior of Fiber Glass Reinforced Concrete Beams", ASCE Journal of the Structural Division, Vol 97, No. ST9, September 1971.

12. Ogaili, A. A. F., Abdulla, F. A., Al-Sabbagh, M. N. M., & Waheeb, R. R. (2020, November). Prediction of Mechanical, Thermal and Electrical Properties of Wool/Glass Fiber based Hybrid Composites. In IOP Conference Series: Materials Science and Engineering (Vol. 928, No. 2, p. 022004). IOP Publishing.

13. Pilakoutas, K., Guadagnini, M., Neocleous, K., & Matthys, S. (2011). Design guidelines for FRP reinforced concrete structures. Proceedings of the Institution of Civil Engineers-Structures and Buildings, 164(4), 255-263

14. Schober, K., Harte, A., Kliger, R., Jockwer, R., Xu, Q., Chen, J. (2015). FRP Reinforcement Of Timber Structures. Construction and Building Materials, (97), 106-118. https://doi.org/10.1016/j.conbuildmat.2015.06.020

15. Teng, J., Yuan, H., Chen, J. (2006). FRP-to-concrete Interfaces Between Two Adjacent Cracks: Theoretical Model For Debonding Failure. International Journal of Solids and Structures, 18-19(43), 5750-5778. https://doi.org/10.1016/j.ijsolstr.2005.07.023

16. Worner V. J (2015). Use of Glass Fibre Reinforced Polymer (GFRP) reinforcing bars for concrete bridge decks. Department of Civil and Natural Resource Engineering. University of Canterbury New Zealand 2015

17. Zaman, A., Gutub, S., Wafa, M. (2013). A Review On FRP Composites Applications and Durability Concerns In The Construction Sector. Journal of Reinforced Plastics and Composites, 24(32), 1966-1988. https://doi.org/10.1177/0731684413492868